JOURNAL OF GEOPHYSICAL RESEARCH, VOL. 88, NO. B12, PAGES 10,495–10,507, DECEMBER 10, 1983

Seismicity and Aseismic Slip Along the Eltanin Fracture Zone

LISA M. STEWART[1] AND EMILE A. OKAL

Department of Geology and Geophysics, Yale University

The seismic history of the Eltanin Fracture Zone on the Pacific-Antarctic Ridge for the years 1920-1981 shows that the seismic slip accumulated during this recording interval accounts for only a small fraction (less than 10%) of the amount of slip predicted by kinematic models of plate motion. We propose that the remainder of the plate motion along the transform faults making up the Eltanin system occurs as aseismic creep. This property singles out the Eltanin among transform systems, where previous studies have found good agreement between seismic slip and predicted rates of motion. The absence of record of any gigantic earthquakes and the geometry of the fault area reduce the likelihood of the Eltanin rupturing along its entire length. We interpret the Eltanin Fracture Zone in the light of an "asperity" model, involving small, well-separated asperities. Its segmented nature and creeplike behavior may be due to the presence of excess magma and, possibly, local upwelling, which could also be involved in the mechanism of generation of the Louisville Ridge.

INTRODUCTION

One of the triumphs of the theory of plate tectonics has been the explanation of the global seismicity pattern: In this framework, interplate earthquakes have generally been used to reveal and confirm information about the velocity and direction of motion of adjacent plates; specifically, the azimuths of transform faults (TF), as determined from bathymetry and slip vectors of earthquakes, constitute key evidence in constraining the direction of local plate motions, and thus the position of poles of relative motion, in models of present-day plate motions such as *Minster and Jordan*'s [1978].

On the other hand, values of plate speeds were obtained exclusively from young magnetic anomalies, averaged over a few million years, and independently from any quantitative estimates of earthquake sizes. It was then shown that along many subduction zones (exemplified by South America) the amount of motion required by kinematic models is indeed accommodated by slip during large earthquakes [*Kanamori*, 1977*a*]. However, in the western Pacific, significant discrepancies between predicted and observed slip led Kanamori to conclude that a large portion of the expected slip occurs "aseismically", either by creep or during extremely slow seismic events that escape detection in the usual seismic frequency band; such plate boundaries include the Mariana trench and, to a lesser extent, the Kurile arc. *Ruff and Kanamori* [1980] interpreted such different regimes as indicative of a variation in the degree of coupling involved at the subduction zone. Similarly, tectonic motion along the San Andreas fault at the boundary between the Pacific and North American plates can be accommodated through seismic events or aseismic creep, depending on the particular section of fault involved [*Allen*, 1981].

Along oceanic transform faults, there is generally good agreement between spreading rates given by models of plate kinematics and the cumulative slip released during large earthquakes. *Kanamori and Stewart* [1976] report such an agreement along the Gibbs Fracture Zone (FZ), *Brune* [1968] sets conditions for agreement along the Romanche and Jan Mayen TF's, and *Stewart and Okal* [1981] conclude that along the Romanche, Conrad, and Bullard TF's, seismic slip accounts for all displacement required by known lithospheric accretion rates. As part of an ongoing investigation of the detailed seismicity of oceanic transform faults, we have found a generally excellent correlation between the cumulative seismic energy released during large TF earthquakes and the amount expected given the length of TF offset and spreading rate [*Stewart*, 1983]. Such a correlation holds for short and long TF's offsetting fast and slow spreading ridges along most mid-ocean ridges. A notable exception is the general area of the Eltanin Fracture Zone system: along this portion of the boundary between the Pacific and Antarctic plates, we find that the amount of displacement inferred from the sparse seismicity is insufficient to account for the amount expected from ridge spreading and suggests that 90-95% of the slip is expressed through aseismic rupture or creep. This paper reports this anomalous character of the Eltanin FZ system, and attempts an interpretation of the deficiency in seismicity in terms of a physical model.

[1]Now at Department of Geological Sciences, Brown University.

Paper Number 3B1073.
0148-0227/83/003B-1073$05.00

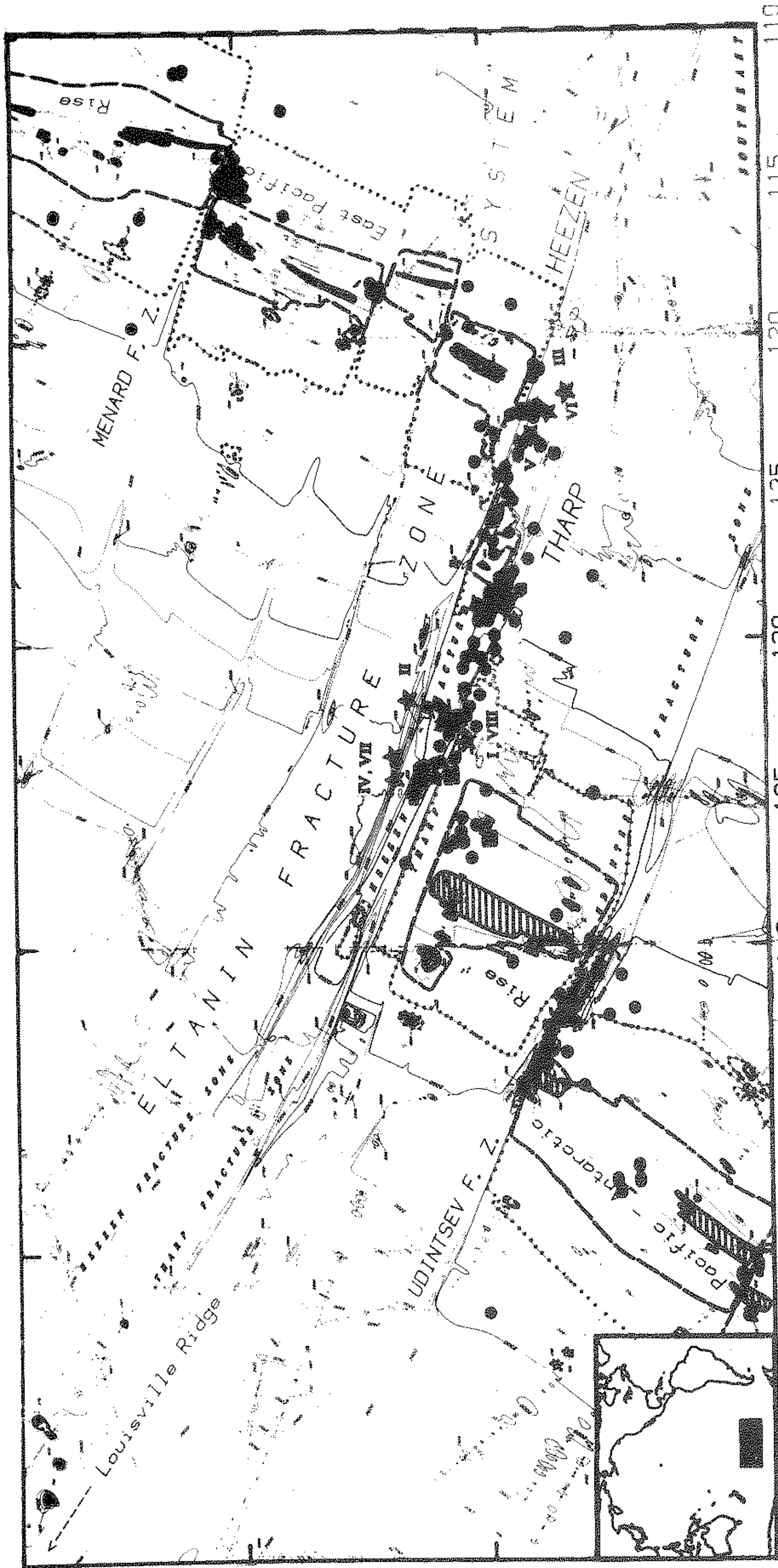

Fig. 1. Map of the seismicity of the Eltanin Fracture Zone area, compiled for the period 1920-1981. This is a Mercator projection, adapted from the bathymetric map of *Mammerickx et al.* [1975]. The 1800, 1600, and 1400 fathom contour lines have been outlined to emphasize ridge segments and seamounts. Individual dots are epicenters from the catalog in Table 1. Stars identify events I-VIII. Inset at bottom left locates the Eltanin FZ in the Pacific.

MORPHOLOGY OF THE ELTANIN FRACTURE ZONE SYSTEM

The Eltanin Fracture Zone system is a major bathymetric feature located between 54° and 56°S and 122° and 134°W, which creates the longest offset of the Pacific-Antarctic Ridge (PAR) (Figure 1). The bathymetry clearly delineates two distinct transform faults separated by approximately 100 km, the Heezen and Tharp TF's [*Mammerickx et al.*, 1975]. Bathymetric and magnetic evidence show that the total offset expressed by the Eltanin FZ is about 1000 km and has been so for the last 70 m.y. [*Weissel et al.*, 1977]. Paleoreconstructions of the plate boundaries in this region [*Molnar et al.*, 1975] show that between 60 and 40 m.y. ago, the South Pacific experienced a major reorientation of plate motion. In particular, during the times of magnetic anomalies 18 to 6, the small NW-SE trending left-lateral TF's south of New Zealand were deactivated, and small, right-lateral, TF's were created south of the Udintsev TF, offset in a nearly E-W direction. The change in spreading direction was accompanied by changes in the morphology of the Eltanin FZ system: the faults composing the Eltanin FZ were "squeezed" together as their azimuth changed from NW-SE to practically E-W and their spacing decreased from 200 to 100 km.

If this reorientation process is still going on, as proposed for example by R.G. Gordon, (personal communication, 1982), horizontal compression in a direction nearly perpendicular to the strike of the FZ should affect the region [*Molnar et al.*, 1975]. From a purely morphological point of view, the faults of the Eltanin FZ system would then be expected to be strongly coupled according to the model developed by *Ruff and Kanamori* [1980] for subduction zones. We will see that the seismic record rules out application of such a model along the Eltanin FZ.

In their global model of plate kinematics, *Minster and Jordan* [1978] assign high importance to data from the Pacific-Antarctic plate boundary and also point out that this relative rotation vector is one of the best constrained. They report, however, that in the region north of the Eltanin FZ, the observed rates are slightly greater than those predicted by their model, the observed rate of 9.8 ± 0.5 cm/yr being modeled by 9.10; south of the Eltanin FZ observed rates of 8.8 ± 0.5 cm/yr are modeled as 8.54 cm/yr, and along it, the model gives 8.9 cm/yr, which is close to the observed value of 9.1 ± 0.5 cm/yr. We will use a value of 9 cm/yr (full rate) as an average of the slip rate along the Heezen and Tharp TF's. According to geometric considerations detailed below, the high spreading rate and the exceptional length of the offset combine to provide the two TF's with the total potential for one $M_w = 7$ event per year. As shown in the next section, the observed seismicity falls considerably short of this level, a result first mentioned by *Brune* [1968], on the basis of a study restricted to a short period of time predating development of the WWSSN.

EARTHQUAKE CATALOG

Table A1[1] is a compilation of all earthquakes occurring in this region from 1920 to 1981, obtained from the NOAA epicentral tape, additional International Seismological Summary (ISS) and International Seismological Center (ISC) listings, and recent Preliminary Determination of Epicenters (PDE) bulletins. Table 1 is a subset of the catalog in Table A1, including only events for which at least one reported magnitude reaches 6. Epicenters are shown as individual dots on Figure 1; a number of events studied in more detail below are identified by roman numbers in the tables and are highlighted by stars on Figure 1.

Location

Events prior to 1960 having magnitudes 6 or greater that were not initially placed on transform faults were relocated using ISS or ISC arrivals, and their magnitudes reevaluated. Recent epicenters located by the ISC are given with a typical 10-km precision for a magnitude 5 event. Careful relocation of older epicenters involved precisions of 25 km at the magnitude 6 level. As shown on Figure 1, the seismic foci define the traces of the two transform faults: the 350-km long Heezen TF and the 650-km long Tharp TF are separated by less than 100 km and are seismically active along their entire lengths. The largest ($M_s \geq 6.5$) events occurring on the Eltanin system are clustered at the eastern end of the Heezen TF and at the western end of the Tharp TF, where the contrast in age, and therefore in thickness and physical properties, is greatest; although one could expect the largest earthquakes to occur in the middle of individual TF segments, where the zone of contact between the two plates is widest, a similar pattern of epicentral clustering of major events at their ends has been reported elsewhere [*Kanamori and Stewart*, 1976; *Stewart*, 1983].

Depth

Because of the generally remote character of the epicentral area (the Eltanin FZ is indeed close to the point at sea farthest away from any land shore) and of the absence of nearby stations, P wave travel times cannot resolve hypocentral depths. Thus, we used long-period body wave modeling [*Stein and Kroeger*, 1981]

[1]Table A1 is available with entire article on microfiche. Order from American Geophysical Union, 2000 Florida Avenue N.W., Washington, DC 20009. Document B83-006; $2.50. Payment must accompany order.

TABLE 1. Earthquakes Occurring in the Region 45° to 60°S by 110° to 155°W, Within 200 km of the Plate Boundary, Between 1920 and 1981, With at least one Magnitude Reported ≥ 6

Date	Time	Epicenter		Magnitudes				Location	Remarks
	UT	°S	°W	m_b	M_s^r	M_s^c	Other		
Feb. 16, 1929	1923:16.0	56.	121.				6.25PAS	H	
Jan. 6, 1930	2350:00.0	55.	131.				6.00PAS	T	
June 15, 1930	2108:11.0	46.	116.				6.25PAS	TF	
Aug. 2, 1930	1606:05.0	57.	135.				6.50PAS	i	*
March 10, 1932	0517:47.0	55.	135.				6.50PAS	T	
July 21, 1932	1616:03.0	55.	131.				6.00PAS	T	
April 19, 1933	0145:47.0	51.	116.				6.00PAS	M	
June 6, 1934	0318:34.0	56.	140.				6.25PAS	U	
Oct. 10, 1934	0954:55.0	48.	116.				6.25PAS	M	
May 16, 1935	2041:30.0	55.	123.				6.25PAS	H	
Aug. 13, 1937	1147:38.0	56.5	130.				6.00PAS	T	
Sep. 5, 1938	1442:32.0	55.	152.				6.00PAS	U	
Jan. 20, 1940	0958:00.0	54.5	132.5				6.75PAS	T	event I
Feb. 14, 1941	1855:16.0	53.5	131.				6.50PAS	FZ ext.	event II
Nov. 13, 1943	1643:28.0	55.	129.			6.2	6.50PAS	T	
April 1, 1944	0922:08.0	57.	128.			6.2	6.00PAS	T	
Sep. 3, 1944	1911:29.0	57.	122.			6.9	7.00PAS	FZ ext.	event III
Jan. 21, 1951	0652:41.0	55.	136.5			6.5	6.88PAS	T	
Aug. 2, 1951	1016:00.0	50.	115.				6.50PAS	M	
May 20, 1953	0745:24.0	53.2	134.			6.2	7.25PAS	FZ ext.	event IV
June 5, 1956	0559:41.0	51.	112.5				6.25PAS	M	
Oct. 19, 1956	1405:34.0	55.86	122.46				6.50PAS	H	
Nov. 4, 1958	2254:46.0	50.	115.				6.00PAS	M	
Mar. 13, 1966	1758:34.5	55.5	126.5	5.5			6.20BRK	H	
Jan. 21, 1967	0254:00.4	49.854	114.891	5.4			6.75PAS	M	
Aug. 18, 1969	0104:04.7	56.022	123.367	5.1	6.4	6.2		H	event V
Aug. 24, 1970	1230:19.5	56.587	142.483	5.9	6.4		6.5PAS	U	
Nov. 3, 1970	0923:04.5	49.985	114.415	5.2	5.8		6.30PAS	M	
Mar. 26, 1971	0908:06.6	55.439	129.100	5.7	6.0			T	
Apr. 4, 1971	1015:37.2	56.245	122.459	6.2	6.6	6.5	6.8	H	event VI
May 7, 1972	2206:30.1	53.713	134.214	5.4	6.3			FZ ext.	event VII
Aug. 7, 1973	0639:00.8	54.351	136.550	5.4	6.1		5.90BRK	T	
Sep. 18, 1973	1332:51.5	54.518	132.624	5.3	6.4	6.2	6.30BRK	T	event VIII
June 25, 1974	0505:19.0	54.642	131.616	6.1	5.7			T	
June 3, 1978	0457:12.5	57.096	140.888		6.0			U	
March 12, 1979	0638:11.7	56.077	122.440	5.4	6.1		5.90BRK	H	

Locations are: T, Tharp TF; H, Heezen TF; M, Menard TF; U, Udintsev TF; TF, other TF; FZ ext., event located on a FZ, outside its expected active segment; and i, intraplate event not located on a FZ. Magnitudes are M_s^c, 20-s M_s recomputed in this study; M_s^r, 20-s M_s reported (ISC); other reported magnitudes are PAS, Pasadena, BRK, Berkeley, and MAT, Matsushiro.

Asterisk indicates event not used in the seismicity budget.

to investigate the depths of the largest events. Following the technique of *Wiens and Stein* [1983], we use the simple model of a homogeneous half space to generate the wave shape resulting from the interaction of direct P, pP and sP for a variety of source depths, and compare it to the data. Results indicate that all depths in the region are less than 20 km and a few are very shallow, around 3 km. In most cases we find the depth to be less than 5 km. Figure 2 shows typical long-period vertical records from a range of stations and compares wave shapes with forward modeled synthetics. Note that in some cases, multiple reflections in the oceanic layer may give added structure to the second swing of the P wave, but in all cases leave the first swing untouched.

Focal Mechanisms

As expected from plate kinematics, all the events located on the Heezen and Tharp TF's have left-lateral strike slip focal mechanisms: P wave polarities for all events in Table A1 with $m_b \geqslant 5$ were collected from ISC bulletins and those occurring on TF's were found to be compatible with left-lateral strike slip on a vertical fault striking 110°. The few exceptions to strike slip mechanisms in this area were some smaller events near longitude 127°W, where a very short spreading ridge is probably present.

Of the largest events located "off-transform", Events III (September 3, 1944; M_s = 6.9) and IV (May, 20 1953; M_s = 6.2) are compatible with left-lateral strike slip, on the basis of first-motion reports, although their mechanisms cannot be fully constrained because of a general paucity of data.

Magnitudes

The striking features of our seismicity list are the rare occurrence of $M_s \geqslant 6$ earthquakes and the absence of $M_s \geqslant 7$ earthquakes in a region expected to be rich in such events. In order to quantify the seismicity of the Eltanin area, we investigated in detail the magnitudes of the earthquakes along the Heezen and Tharp TF's. For older events we used Gutenberg's microfilmed notepads [*Seismological Society of America,* 1980] and original records obtained from old long-period stations. Whenever possible, and in order to minimize problems related to instrument responses, we used direct comparisons with records, at the same stations, of more widely recorded events of well-determined magnitudes.

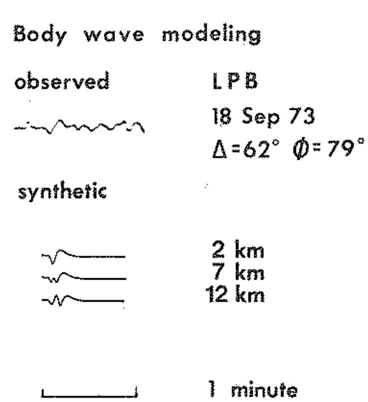

Fig. 2. Determination of hypocentral depth of event V through body wave modeling. The top trace is the observed long-period pulse of the signal that is rapidly distorted by depth phases, even for depths of only 7 km. The depth of this event is thus constrained to no deeper than 5 km.

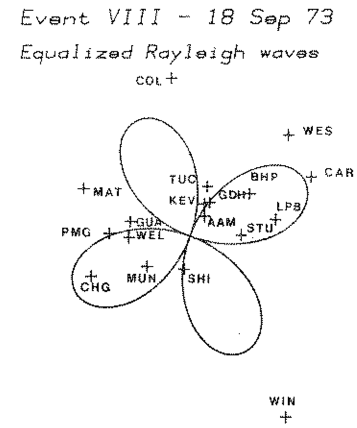

Fig. 3. Example of equalized Rayleigh waves, used to determine the static (in fact, long-period) magnitude M_w, following the technique of *Kanamori* [1970, 1977*b*]. Solid line is theoretical amplitude radiation pattern, crosses individual data points with station code shown.

In order to make estimates of the cumulative seismic moment released over several decades we need to compare the sizes of old and new events that have been recorded on different kinds of instruments, whose responses were peaked around different periods. Toward this goal, we first conducted detailed investigations of the magnitudes, measured at various periods, of some of the larger, recent events well recorded on the WWSSN. We obtained the standard m_b at 1 s, and M_s at 20 s from original records and computed the energy magnitude M_w [*Kanamori,* 1977*b*] from equalized long-period Love and Rayleigh waves, following the techniques of *Kanamori* [1970]. Figure 3 is an example of this technique, applied to Rayleigh waves from event VIII. For very shallow, pure strike slip focal mechanisms it is easily shown that the inferred value of the moment is stationary with respect to an error on the depth. Resulting values of M_w are typically representative of energy in the 70-s range. The following is a list of the most significant recent events on the Eltanin system.

Event V: Heezen FZ, August 18, 1969; 56.02°S, 123.37°W; m_b=5.1, M_s=6.4 . There is noticeable discrepancy between body and surface wave magnitudes for this event, indicating that there may be preferential energy release at long periods. From long-period Love and Rayleigh waves we obtain a seismic moment of 3.5 × 10^{25} dyn-cm with fault strike ϕ=110°, dip δ=90°, and slip λ=0. This yields M_w=6.3, indicating that the surface wave magnitude is an adequate measure of the energy released during the event: the earthquake is not significantly slower than 20 s.On the other hand, the small value of the body wave magnitude is intriguing. Figure 4 shows portions of the South Pole short period and Bogota, Colombia, long-period P wave records, as well as horizontal records of the Rayleigh waves at Arequipa, Peru. Individual magnitudes computed from

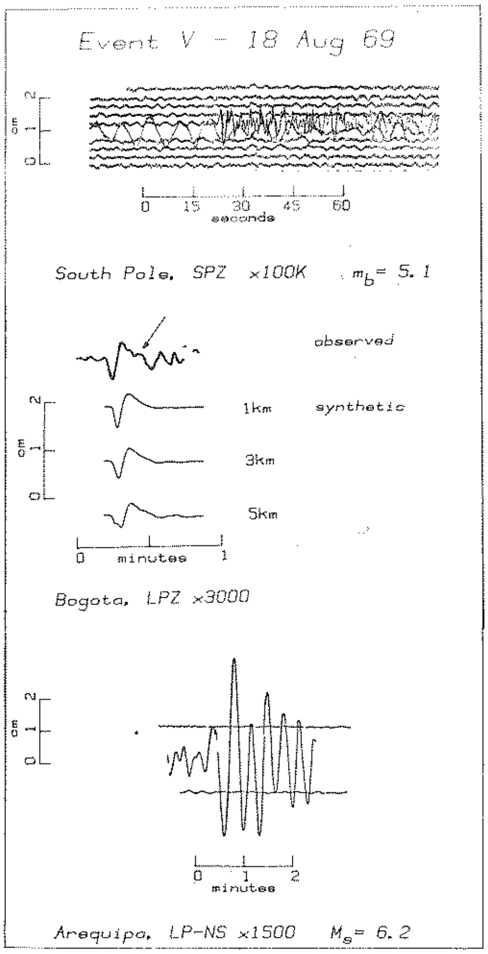

Fig. 4. Seismograms of event V (August 18, 1969). (top) Short-period vertical record at South Pole (Δ = 34.07°). (center) Long-period body waves observed at Bogota (Δ = 72.68°) and modeled for different depths, including the influence of water reflections. Note (arrow) later arrivals, requiring more complex source function. (bottom) Horizontal Rayleigh wave record at Arequipa, Peru (Δ = 55.55°). Note evident discrepancy between m_b and M_s.

these records are also given. In other cases of TF earthquakes that exhibit similar m_b:M_s disparity, it was usually found that the trace of the P wave on long-period records reveals a complex rupture pattern that cannot be modeled by a single arrival [*Okal and Stewart*, 1982]. Similarly, in the present case and as shown by the long-period body wave modeling at Bogota, it is not possible to account for the later structure present in the P waves with a simple source, even including the influence of water reflections. The complexity of rupture is expressed in a later arrival (see arrow on Figure 4) that contaminates the first waveform and gives the source a long-period source time constant. The combined effects of small multiple sources can explain the coexistence of tiny body waves and sizeable surface waves. Because M_w and M_s are not significantly different, this may be an example of a slow event involving only a small rupture area but still featuring complexity in the source.

Event VI: Heezen FZ, April 4, 1971; 56.25°S, 122.46°W; m_b=6.2, M_s=6.6 . The equalized long-period surface wave radiation patterns are compatible with the first motion focal mechanism and give a moment M_o=8 × 10^{25} dyn-cm for strike slip motion on a vertical fault striking 110°. *Molnar et al.* [1975] give the slightly different solution ϕ=120°, δ=90°, λ=10°, for which the equalized moment would be similar. M_w = 6.5, indicating that again for this event the magnitude measured at 20 s is an adequate measure of the energy released. Short period P waves from Tucson and long-period Love waves from Ann Arbor are shown in Figure 5. Long period P waves were found to exhibit no special complexity or anomalously long nature; in the classification of *Okal and Stewart* [1982] this is considered a fast earthquake: this time, m_b is not significantly smaller than M_s, especially in view of the expected saturation of m_b around 6.3 [*Geller*, 1976].

Event VIII: Tharp FZ, September 18, 1973; 54.52°S, 132.62°W; m_b=5.3, M_s=6.4 . This is the largest event recorded by the WWSSN on the Tharp TF. The obvious discrepancy between m_b and M_s warrants further investigation into possible low-frequency content in the

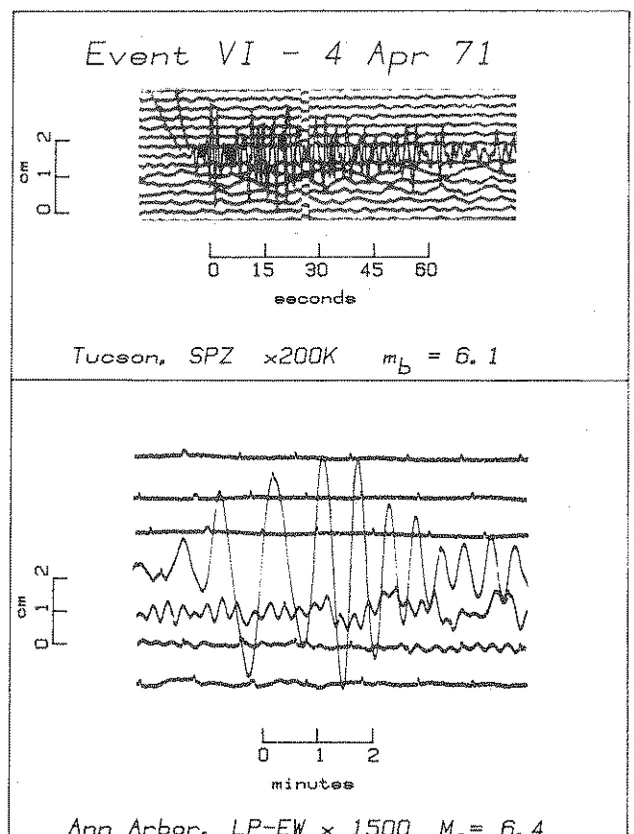

Fig. 5. Seismograms of event VI (April 4, 1971). (top) Short-period P wave record at Tucson (Δ = 88.80°). (bottom) Love waves at Ann Arbor, Michigan (Δ = 103.72°). Comparison with Figures 4 and 6 shows obvious difference in m_b:M_s, this event being of the regular, "fast" type, while events V and VIII are of the "slow" type.

source time function. Equalized long-period Love and Rayleigh waves yield a seismic moment of 3×10^{25} dyn-cm for left-lateral strike slip on a vertical fault striking 113°. This corresponds to M_w=6.3, comparable to the confirmed M_s=6.4. Figure 6 shows short period records at Tucson in the same geometry and recording conditions as for event VI. The difference in m_b between the two events is striking. Low-amplitude body waves are present on some long-period records (e.g., Caracas, Figure 6); the first pulse exhibits a width and structure representative of an ordinary rupture process. As opposed to the case of event V, wave shape modeling suggests that structure in the second pulse is due to water reflections [*p(nw)P*], rather than to complexity of the source. While the m_b:M_s anomaly for this event definitely makes it a slow earthquake, it does not feature the characteristics of a complex rupture history.

MAGNITUDES OF OLDER EVENTS

As shown by *Geller and Kanamori* [1977], the accurate investigation of older events is made possible by the recognition that *Gutenberg*'s [1957] unified magnitude m is comparable to present-day M_s, if measured at a period approaching 20 s. We obtained all available records of the few 1920-1960 events whose magnitudes were thought to be 6.25 or greater in order to confirm or reevaluate their sizes. Gutenberg magnitudes of smaller events were taken to be representative of M_s.

Present-day magnitudes are measured at two different periods: 1-3 s (m_b), and 20 s (M_s). In most cases, reported magnitudes for the older events were calculated from maximum amplitudes of waves recorded on instruments with gains peaked at 10-12 s, and need not be comparable to either m_b or M_s. By computing instrument responses at 20 s and measuring the 20-s waves, we obtained M_s for some older events. Usually, there are substantial discrepancies between magnitudes measured at different periods; this may be a real effect due to the source time function or may be the result of a poorly known response function of the instrument. For example, event III was given an m = 7.0 by *Gutenberg and Richter* [1954], but comparison of original records gives a wide variety of magnitudes, as is often the case even for present-day M_s. Amplitudes of 20.0-s waves from Honolulu give M_s = 7.2, 16.8-s waves from College give M_s = 7.2, and 24.0-s waves from San Juan give M_s = 5.8. For Event II (February 14, 1941), results from analyses of records from the San Juan Wenner instrument (peak gain at 10 s) range from M_s = 6.7 at 28 s to M_s = 5.4 at 13 s. *Gutenberg and Richter* [1954] report m = 6.5 for this event. Overall, our average magnitudes were comparable to those published by Gutenberg and Richter. Of the 18 events we tested, only one (event IV, May 20, 1953) was found to have more than 1/3 unit difference with these authors' values.

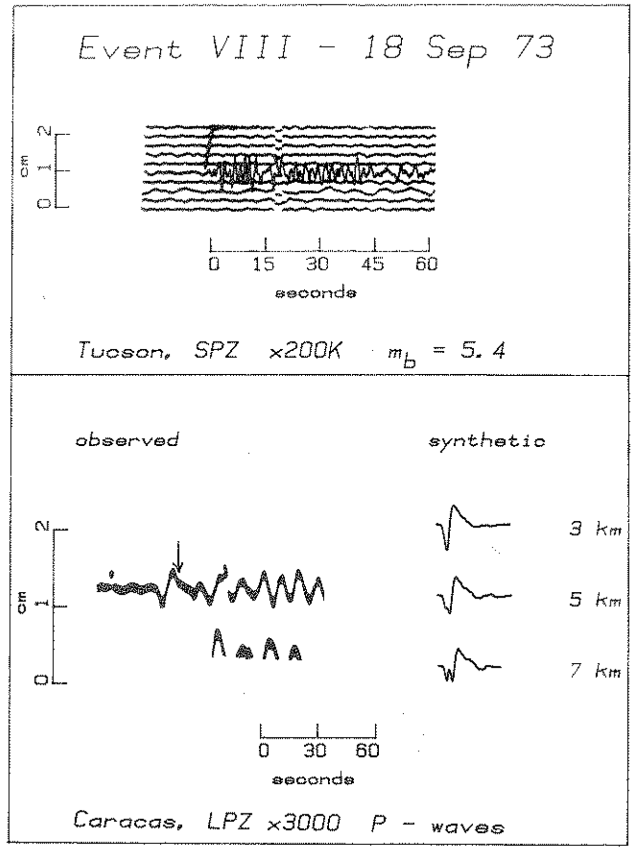

Fig. 6. *P* wave seismograms of event VIII (September 18, 1973). (top) Short-period record at Tucson (Δ = 88.65°). (bottom) long-period *P* waves at Caracas (Δ = 84.95°), compared to synthetics obtained by including *P*, *pP*, *sP* and multiple water reflections. Note excellent agreement between observed and theoretical wave shape for a very shallow source (3 km below ocean floor). Any deeper source, as shallow as 5 km, would result in a significant distortion of the first downswing due to strong excitation of *pP* and *sP*. Later structure (arrow) is due to water reflections in the 3.5-km ocean column.

THE BUDGET OF SEISMIC MOMENT RELEASE

For large recent events we have shown that an upper bound on the seismic moment may be calculated from M_w, and that M_w itself is well represented by M_s. This is in contrast with the case of the Gibbs TF discussed by *Kanamori and Stewart* [1976]. In order to get an estimate of the amount of energy being released along the Eltanin FZ, we computed the cumulative seismic moment release rate as follows.

For events prior to 1953, Gutenberg's revised magnitudes m are usually compatible with M_s [*Geller and Kanamori,* 1977]; the published magnitudes were checked against Gutenberg's notepads [*Seismological Society of America,* 1980] and taken to correspond to M_s

at 20 s.For later events, usually only m_b was listed. To allow for the possibility that m_b is less than M_s, we added 0.5 to every m_b and took the result to represent M_s, unless M_s or a station magnitude (e.g., M_{PAS}) was given. We generously assigned M_s=5.5 to those events whose origin times and epicenters were reported without magnitudes. Events that could be constrained to lie within 100 km of the mapped transform faults were considered to contribute to the seismicity of the FZ system, even though several such earthquakes are strictly intraplate (e.g., event II). Since our investigation of recent earthquakes has failed to reveal events with source time functions slower than 20 s, M_s was then set equal to M_w for the purpose of calculating the seismic moment M_o.

Summing up moments for all Eltanin events of $M_s \geqslant 5$, from 1920 to 1981, we get 1.3×10^{27} dyn-cm, or approximately 2.1×10^{25} dyn-cm/yr, highlighting the paucity of magnitude 6 events in the seismicity list. This figure is then compared to the expected seismic moment rate defined as

$$\dot{M}_o = \mu \ v \ A \tag{1}$$

where $\dot{M}_o$ is the moment release rate, μ the rigidity along the fault, v the (full) kinematic slip rate, and A the area of faulting. Since we are dealing with young oceanic lithosphere, we take a reasonably low rigidity $\mu = 3 \times 10^{11}$ dyn cm^{-2}. We estimate the transform contact area, A, by using *Stein*'s [1978] model:

$$A = (2/3) \ C \ (l^3/v)^{1/2} \tag{2}$$

where C is the constant of thickening of the lithosphere with square root of age (C = 8 km/(m.y.)$^{1/2}$), l is the length of the transform fault segment, and v is the full spreading rate. Using the geometric relation

$$h = C \ (l/v)^{1/2} \tag{3}$$

with the following geometric parameters (l = 1000 km, v = 9 cm/yr), Stein's model gives a maximum fault depth of 27 km, in the single fault case, and if the FZ system is treated as two transforms, values of 16 km for the Heezen TF and 21 km for the Tharp TF; these values are in good agreement with the maximum reported depth of 20 km. The corresponding total area of contact is 17,800 km^2 (single fault), slightly reduced to 13,000 km^2 if we break up the system in its two transforms. With a plate speed (full rate) of 9 cm/yr, we obtain a moment rate of 4.8×10^{26} dyn-cm/yr for the single fault model, and 3.5×10^{26} dyn-cm/yr for the Heezen-Tharp system.

Clearly, the expected moment release rate is at least one order of magnitude greater than observed.

THE DEFICIENCY IN SEISMICITY: DISCUSSION OF THE OPTIONS

Before we can assert that the seismicity is indeed deficient, we must question possible sources of error.

A Gigantic Event to Make up the Difference ?

We must first determine whether or not we are simply "waiting for the big one". Recurrence times of catastrophic earthquakes vary regionally, and a value of 150 years is typical. Some areas, such as the Alaska peninsula may have much greater recurrence times [*Sykes*, 1971], considerably longer than the extent of our observation period in unpopulated areas as remote as the Eltanin FZ. We have chosen to limit this study to events posterior to 1920, since this corresponds to the starting date of detailed ISC bulletins. However, the seismic station at Wellington, New Zealand, started in 1898, and thus the possibility of a gigantic event escaping detection during the years 1898-1920 is very remote. Indeed, in their compilation of turn-of-the-century seismicity going back to 1896, *Kanamori and Abe* [1979] do not mention any large earthquakes in the Eltanin region nor does *Abe* [1981] in his compilation of shallow seismicity for the years 1904-1980. If a giant Eltanin earthquake is to release the strain accumulated since 1896, the resultant slip would be 8 m, generating an M_w = 8.2 event. There is no historical evidence that an event of that size has ever occurred in this area. Furthermore, it is extremely unlikely that such a strain could accumulate over the shallow, ribbonlike area of a fast spreading TF: The largest earthquake recorded on an oceanic TF is the 1942 M_w = 8.0 event on the Prince Edward Island TF, southeast of Africa (E.A. Okal, unpublished data). TF's in that area commonly experience very large earthquakes to accomodate completely the slip predicted by kinematic models. This is made possible by the large width of the fault, itself a result of the very slow spreading rate of the Southwest Indian Ocean Ridge (1.5 cm/yr full rate), a situation opposite to that in the Eltanin area.

Include Many Small, Undetected Events?

The location of the Eltanin FZ makes for a nightmare in seismic detection thresholds. Magnitudes reported in recent PDE bulletins for Eltanin events can be as low as m_b = 4.6. However, and for the purpose of this discussion, we will conservatively estimate that our catalog is complete only down to one unit greater than this, around m_b = 5.6, for the years following 1963, but that we miss few events with m_b > 5.3. This estimate is based upon detection capabilities of the high-gain WWSSN stations at Scott Base, Charter Towers, and La Paz. We could, in principle, account for the apparent deficiency in seismicity by assuming that approximately 250 m_b = 5.3 events go undetected each year in this region. However, such seismicity would be detected by the high-gain station at South Pole and those of the French Polynesia Seismic Network, centered on Tahiti, only 4000 km to the north [*Okal et al.*, 1980]. Conceivably, events of an even lower magnitude, and in even larger numbers, could also do the job. However, the problem would then arise why such seismicity occurs exclusively at such low magnitude levels; the discrepancy between seismicity at the magnitude 4 and 6 levels would require b values larger than 2, observed only during episodes of volcanic activity. Although we cannot entirely discard the possibility that the deficient motion is taken up by a multitude of events in the magnitude 3-4 range, we prefer the limiting model of creep: a continuous process involving an infinite number of events whose moment goes to zero.

Change the Global Models ?

In a further effort to explain the discrepancy between observed and expected seismicity in the Eltanin region, we might question the validity of the parameters used in (1). We have taken the rate found by *Minster and Jordan* [1978], which should be accurate to within 10-20% [*Molnar*, 1979]; changing to another model of plate motions, such as *Chase*'s [1978] would not significantly affect the predicted rates. Equations (1) and (2) show that the slip rate should be decreased 100 times to reduce the moment rate by an order of magnitude; this is clearly impossible. It would also be unreasonable to propose a rigidity one order of magnitude lower (say 3×10^{10} dyn/cm^2); even to divide it in half verges on treating the oceanic lithosphere as sedimentary.

An Evolving Plate Geometry or a Delocalized Plate Boundary ?

The entire region of the Eltanin FZ system may be a broad zone of deformation instead of two discrete TF's. There is evidence for moderate "intraplate" seismicity along the extensions of the TF's, where according to the principles of rigid plate tectonics there should be none. The largest event recorded in the area is event III (September 3, 1944; 56.5°S, 122.2°W; M_s = 6.9). This relocated epicenter is on the Tharp FZ, 300 km east of its TF segment, and 100 km to the south of the Heezen TF. The event cannot be placed on what should be the active section of the Heezen TF without increasing the standard deviation of the travel time residuals to an unreasonable 9 s, using 16 stations, versus 2.5 s for our preferred location, a figure typical of our relocation efforts for old events in remote areas, when this number of stations is used.

Several other events have occurred on both the eastern and western extensions of the Tharp and Heezen TF's, respectively, indicating that motion between the Pacific and Antarctic plates may take place along a more diffuse boundary than previously modeled. We have documented recent, precisely located events (e.g., event VII), as well as older shocks, ruling out the possibility that this intraplate seismicity could be an artifact of poor relocations.

These epicenters are not spread over the entire intertransform region; rather, they are concentrated at the east and west ends of the FZ system, along portions of the Heezen and Tharp TF's that should be sutured. These "intraplate" events appear to align with the southward and northward extensions of the PAR and could be the expressions of propagation of the ridge system across the Eltanin FZ, as in models by *Hey* [1977] and *Hey and Wilson* [1982]. *Farmer et al.* [1982] have proposed similar models to explain large-scale intraplate seismicity in the Scotia Sea region and made a case for microplate formation and/or propagating rifts. Given the geometry of the Eltanin FZ system, such rift propagation could result in the cessation of motion along one of the TF's, with all the required slip being taken up by the second one. In order to determine whether either of the TF's is trying to dominate the other, we assess their seismic moment rates individually. We do note that when seismic moment rates are computed for the two TF's separately for the years 1960-1980 (a period in which the seismic moment rate matches the long-term average rate), we find 1.85×10^{26} dyn-cm or 9.2×10^{24} dyn-cm/yr for the Heezen TF (9% of the seismic moment rate required by the kinematic model) and 1.5×10^{26} dyn-cm or 7.3×10^{24} dyn-cm/yr for the Tharp TF (3% of the seismic moment rate required). In this respect, the Tharp TF is even more anomalous than the Heezen, but the difference in levels of activity along the two TF's is not significant; we could not say that one TF has taken over and left the other sutured. Note also that all events (including those not located on the expected segments of activity of the two FZs) were taken as contributing to the seismic budget; their character as regular TF events or anomalous, "intraplate", shocks will not help solving the seismic deficiency.

It is also important to stress that no large-scale intraplate seismicity occurs north of the Eltanin Fracture Zone system in the Pacific Plate [*Greenberg and Okal*, 1983] or south of it in the Antarctica plate [*Okal*, 1981]. In this respect, the situation along the Eltanin FZ is quite different from that on the Southeast Indian Ocean Ridge, between Australia and Antarctica, where *Stewart and Okal* [1982] have documented comparable budgets for intraplate and interplate seismicity, involving large-scale deformation of the Australian plate. Thus the seismic deficiency along the Eltanin Fracture Zone system is not an artifact of a "delocalization" of the plate boundary.

An Overestimated Area of Rupture

It is thus clear that the only parameter which we may have overestimated in our computation of the expected seismic moment rate release is the constant A in (1). This has to represent the area of locked contact between brittle sections of lithosphere; the observed seismicity constrains it to being no larger than about 800 km^2. We overconfidently modeled it as the 1100°C isotherm in the simple thermal model of *Stein* [1978]. In the line of recent results by *Wiens and Stein* [1983], the 600°C isotherm may also be considered. However, this choice would reduce the constant C in (2) and (3) only down to 3.7 km/(m.y.)$^{1/2}$, and A to only 6000 km^2; additionally, the value C = 8 km/(m.y.)$^{1/2}$ correctly predicts the output of seismic energy along other TF's (e.g., the Conrad FZ in the South Atlantic [*Stewart*, 1983]).

In order to reduce the area of seismic rupture A to 800 km^2, we can envision two models: A continuous, but very narrow, brittle zone modeled as a thermal boundary, or a series of a few discrete, separate asperities, locking only selected portions of an otherwise creeping fault. The continuous model would require a maximum depth of contact of only h = 1.2 km (if we model the fault as a 1000-km transform; only slightly more for a two-fault system); interpreted as a thermal boundary, this depth would represent a 100°C isotherm for a deep mantle temperature T_m = 1300°C [*Turcotte and Schubert*, 1982, p. 164] or alternatively could fit the 600°C failure of olivine only if T_m was allowed to be 8500°C! Both of these models are clearly unacceptable. It is therefore more likely that the reduced area of brittle contact is made up of isolated asperities.

In the framework of *Lay and Kanamori*'s [1981] model, fast earthquakes (characterized by simple source functions lasting much less than 20 s) correspond to the rupturing of one large asperity and occur on strongly coupled faults with evenly distributed stress accumulation. Among oceanic TF's, the Prince Edward Island TF or the Challenger FZ, with their ordinary rupture characteristics and high-magnitude events, are examples of this end-member-type fault. Such earthquakes represent sudden release of energy along a single large area of high strength. As the distribution of stress concentration becomes nonuniform, the strength of coupling decreases, and the resulting earthquakes have complex source time functions: with smaller, slightly separated regions of coupling, the rupture of one area of stress concentration may trigger another, resulting in the observed complex source time history. Most of the slow earthquakes that have been identified along oceanic TF's fall into this category. Examples are events along the Gibbs, Romanche, Conrad, and Bullard TF's [*Kanamori and Stewart*, 1976; *Okal and Stewart*, 1982]. With even weaker coupling, as the size of the stress concentration areas is reduced and zones of high strength become isolated, the earthquake magnitude decreases, until on a long, smoothly slipping fault, there are no large earthquakes. This is the case of the Eltanin FZ. The degree of coupling is so low that 90-95% of the slip occurs aseismically. The Eltanin FZ may be considered the end-member example of the slow transform fault. Its occasional earthquakes can be "slow" or "fast", depending on whether the rupture can jump to the next area of stress concentration: for example, event VI, a fast earthquake of moment 8 × 10^{25} dynes-cm, could involve an asperity approximately 10 km in radius, while keeping a strain no larger than 10^{-4}. The rupture time of such an asperity would be no more than a few seconds; in the model of an elongated, ribbonlike fault, this earthquake would require at least 80 km of rupture, and the corresponding increase in rupture time would clearly result in an M_s:M_w disparity, which is not observed.

Whether the deformation outside the asperities takes place coseismically, as the result of its extension to a plastic layer constributing no stress drop [*Das*, 1982], or is mainly the result of continuous creep escaping seismic detection, cannot be resolved at this time.

DISCUSSION

The mechanism by which the walls of the Eltanin Fracture Zone have become decoupled, except along a limited number of locked asperities, is not clear. It could involve lateral variations in both the petrology and the thermal regime of the lithosphere; both suggest extraneous magmatic activity, possibly in the form of a hot spot. Along circum-Pacific subduction zones, *Acharya* [1981] has indeed suggested that the degree of aseismicity, or decoupling, is directly related to the amount of volcanic activity. Whether increased volcanism decreases the coupling and results in aseismic slip through the placement of excess, molten, hot material, or conversely, the continuous slipping helps generate more magma through increased friction has not been determined. In the following section, we will review some of the other geophysical data in the context of the speculation that a hot spot may be embedded in the Eltanin system.

Free air gravity data [*Anderson et al.*, 1973] show a gravity high along the East Pacific Rise (EPR) north of the Eltanin FZ. The anomaly reaches +21 mGal; the +20 mGal contour follows the EPR and bends along the northern flank of the Eltanin FZ. The pattern of the gravity profile resembles that of the mid-ocean ridge near the Azores hot spot and also recalls the Amsterdam-St Paul Islands high in the area of the Kerguelen-Heard hot spot in the southeast Indian Ocean. It has been shown that such long-wavelength gravity anomalies must be the result of a deep physical process, often associated with asthenospheric flow [*Anderson et al.*, 1973; *Sclater et al.*, 1975]. Thus it seems likely that a region of mantle upwelling exists in the vicinity of the Eltanin FZ.

On the basis of geoid anomalies derived from satellite altimetry, *Cazenave et al.* [1983] suggest that thermal characteristics of oceanic lithosphere across the inactive sections of the Eltanin FZ (and the Amsterdam FZ in the southeast Indian Ocean) are anomalous with respect to those of the northeast Pacific. They report low values for the lithospheric plate thickness and thermal diffusivity in the vicinity of the Eltanin and Amsterdam FZs. They interpret this thinning of the lithosphere as the result of regional variations in its thermal properties.

It is clear that their method has a long-wavelength resolution and therefore averages the properties of the plate over distances large with respect to the size of the asperities. Thus their model of a "thin plate" would generally be compatible with our results, despite the inability of a very thin plate to sustain fast earthquakes of the type of event VI. However, Cazenave et al. do not specifically involve a hot spot structure in their model.

Finally, any interpretation of the tectonics of the Eltanin FZ area must account for the presence of the Louisville Ridge, a linear bathymetric feature mapped by *Hayes and Ewing* [1971], trending NW-SE and which appears to originate at the western end of the Eltanin FZ. Several interpretations of its origin have been given, although the absence of geochemical data from Louisville Ridge Basalts leave them tentative: Most bathymetric surveys of the South Pacific [e.g., *Mammerickx et al.*, 1975] map the Louisville Ridge as a chain of isolated seamounts as well as recent work based on radar altimetry [*Cazenave and Dominh,* 1983]. On the other hand, *Sandwell* [1982] argues for a continuous feature, possibly comparable to the Ninetyeast Ridge in the Indian Ocean. At any rate, the strong signature of the Louisville Ridge requires formation by a hot spot acting on lithosphere at least 35 m.y. old (J.K. Weissel, personal communication, 1983). In their reconstruction of hot spot trajectories to account for oceanic plateaux and other bathymetric features, *Henderson and Gordon* [1981] have indeed proposed that a hot spot be responsible for the formation of the Ontong-Java Plateau and the Louisville Ridge. Its present location would have to be near the MOR at the Eltanin FZ. This hot spot would then have managed to "capture" the ridge in a way comparable to the history of Iceland [*Vink and Morgan*, 1981]. At this point in history, the Louisville Ridge would become invisible in the geoid. There is indeed some indication [*Sandwell,* 1982; *Dixon and Parke,* 1983] that its signature fades away around longitude 150°W. There would not necessarily yet be a symmetric ridge on the Antarctica plate because of the large length of the Eltanin TF's system.

An on-ridge hot spot located inside a major TF system would create intense volcanism along the walls of the fault. Preliminary results by *Gorodnitskiĭ et al.* [1980] report intense magnetization on the southern flank of the Heezen TF in an area where the southern side is bathymetrically higher. On the basis of the magnetic properties of ultramafic dredged samples, they suggest that there were several stages of magnetization, associated with stages of injection of ultramafic material. However, there are clearly many problems associated with placing a hot spot inside the Eltanin FZ system:

First, the trend in the elevation of seamounts along the Louisville Ridge is in the opposite sense of what would be expected from such a model: the highest elevation is at Valerie Guyot, near the Tonga trench, farthest away from the Eltanin TF's. *Molnar et al.* [1975] have proposed to explain this in the framework of "asthenospheric bumps", which *Menard* [1973] introduced to model the elevation of other island chains in the Pacific. This trend could also be due to a decrease in volcanic activity, indicating that the hot spot has been fading, as *Morgan* [1981] has proposed at other locations; however, this concept is still largely speculative.

The lack of a well-defined seamount or plateau structure on the ocean floor would argue against the presence of an active hot spot at the Eltanin FZ. However, *Vogt* [1976] has proposed that the high spreading rate could prohibit the formation of an Iceland-type feature in this area. But his interpetation of gravity data places the hotpsot at the Udintsev TF, to the south of the Eltanin system. It has indeed been observed that the Udintsev TF is the focus of occasional swarms of T wave activity, recorded in Tahiti, and reminiscent of the activity at confirmed volcanic locations, such as MacDonald Volcano (J. Talandier, personal communication, 1982).

Finally, the location of the hot spot itself remains a major problem. The Louisville Ridge demands it in the Eltanin Fracture Zone; *Vogt* [1976] places it at the Udintsev FZ. Investigations of the seismicity along the Menard and Udintsev TF's show that they share some of the aseismic character of the Eltanin FZ. Our model would have to assume that the influence of the hotpsot can be "felt" several hundred kilometers away. This situation is not impossible due to the proposed existence of large-scale asthenospheric flow away from a hot spot [*Morgan,* 1978], and is even suggested by our earlier study of more strongly coupled, although definitely slow TF's [*Okal and Stewart*, 1982], but remains speculative.

Clearly, the assumption that a hot spot now resides in the Eltanin system is not fully documented, and raises many important problems; however, many observed features in the area would be explained by an increased and sustained magmatic activity. A definite understanding of this region will have to be based on geochemical data and radiometric ages of basalts along the Louisville Ridge.

CONCLUSION

In a previous paper, we had presented evidence that the existence of a hot spot on or near a MOR affects the strength of coupling along long TF's in the vicinity [*Okal and Stewart,* 1982]. Sufficiently long transform faults create offsets along the MOR system that act as barriers to subaxial flow of asthenospheric material produced by a hot spot [*Vogt and Johnson,* 1975]. It is possible that a region of mantle upwelling, "trapped" between the pair of long offsets created by the Heezen and Tharp TF's, could reduce the coupling between the Pacific and Antarctic plates to such an extent that only a small portion of the accumulated strain is released during moderate earthquakes, while the remaining

90-95% is released aseismically. Displacement occurs along the entire length of both the Heezen and Tharp TF's and along portions of their FZ extensions as well.

There are many questions still unanswered concerning the Eltanin FZ system, and there exist several ways of interpreting the geophysical data, even in the light of the seismic evidence we have presented. Our understanding of processes within the oceanic lithosphere would be greatly enhanced with further work on the age of the ocean floor in the Eltanin FZ-Louisville Ridge area and with investigation of the petrologic and geochemical aspects of samples from this region.

In particular, a major question that must be raised is the nature of the differences between adjacent zones of different coupling characteristics along faults. Along all transform faults one would expect areas of slightly different composition or structure due to inhomogeneous processes during accretion at the ridge. However, the interaction of two different sources of magma (hot spot and MORB) could lead to lateral variations in the chemical composition of the walls of the transform: gradients of chemical composition resulting from contamination of MORB's by hot spots have been documented both for on-ridge and intraplate hot spots [*Schilling*, 1973; *Schilling et al.*, 1982], and we have indeed correlated slow earthquakes along a few TF's with reported geochemical anomalies [*Okal and Stewart*, 1982]. Additionally, the presence of a hot spot embedded in the fracture zone system would give rise to rapid lateral variations in heat flow. This could, in turn, act upon the alteration processes of the ocean crust by seawater and strongly affect the nature of coupling between transform fault walls. Although the detailed nature of the factors controlling the coupling along TF's remains unclear, we think that the exceptional seismic characteristics of the Eltanin FZ strongly suggest that extraneous magmatic activity, possibly in the form of a hot spot, takes place in the area.

Acknowledgments. We are grateful to Anny Cazenave, Tim Dixon, Don Forsyth, Richard Gordon, David Sandwell, Seth Stein, Jacques Talandier, Jeff Weissel, and Doug Wiens for discussion over various aspects of this research and for kindly sending preprints of their papers and abstracts. Repeated use of the film chip collection at Lamont-Doherty Observatory is gratefully acknowledged. Records of older events were made available by many colleagues at various observatories. Body wave modeling was performed using a program originally obtained from Seth Stein and Glenn Kroeger. The paper was greatly improved through thoughtful reviews by Seth Stein and Jeff Weissel. This research was supported by the National Science Foundation under grant EAR-81-06106. We also thank Joe Greenberg, who helped in the initial compilation of the seismicity, supported in part by the Office of Naval Research, under contract N00014-79-C-0292.

REFERENCES

Abe, K., Magnitudes of large shallow earthquakes from 1904 to 1980, *Phys. Earth Planet. Inter.*, *27*, 72-92, 1981.

Acharya, H., Volcanism and aseismic slip in subduction zones, *J. Geophys. Res.*, *86*, 335-344, 1981.

Allen, C. R., The modern San Andreas fault, in *The Geotectonic Development of California*, edited by W.G. Ernst, pp. 511-534, Prentice-Hall, Englewood Cliffs, N. J., 1981.

Anderson, R. N., D. McKenzie, and J. G. Sclater, Gravity, bathymetry, and convection in the Earth, *Earth Planet. Sci. Lett.*, *18*, 391-407, 1973.

Brune, J. N., Seismic moment, seismicity, and rate of slip along major fault zones, *J. Geophys. Res.*, *73*, 777-784, 1968.

Cazenave, A., and K. Dominh, Anomalies du géoïde au-dessus de la chaîne sous-marine Louisville Ridge (Pacifique Sud); conséquences possibles sur son origine, *C.R. Hebd. Séances Acad. Sci. Sér. II*, *296*, 487-492, 1983.

Cazenave, A., B. Lago, and K. Dominh, Thermal parameters of the oceanic lithosphere estimated from geoid height data, *J. Geophys. Res.*, *88*, 1105-1118, 1983.

Chase, C. G., Plate kinematics: The Americas, East Africa, and the rest of the world, *Earth Planet. Sci. Lett.*, *37*, 355-368, 1978.

Das, S., Appropriate boundary conditions for modeling very long earthquakes and physical consequences, *Bull. Seismol. Soc. Am.*, *72*, 1911-1926, 1982.

Dixon, T. H., and M. E. Parke, Bathymetry estimates in the Southern Oceans from SEASAT altimetry, *Nature*, *304*, 406-411, 1983.

Farmer, R. A., K. Fujita, and S. Stein, Seismicity and tectonics of the Scotia Sea area (abstract), *Eos Trans. AGU*, *63*, 440, 1982.

Geller, R. J., Scaling relations for earthquake source parameters and magnitudes, *Bull. Seismol. Soc. Am.*, *66*, 1501-1523, 1976.

Geller, R. J., and H. Kanamori, Magnitudes of great earthquakes from 1904 to 1952, *Bull. Seismol. Soc. Am.*, *67*, 587-598, 1977.

Gorodnitskiĭ, A. M., T. I. Lin'kova, and G. L. Kashintsev, Magnetism of deep layers of oceanic crust in the Eltanin fault, *Dokl. Acad. Sci. USSR, Earth Sci. Sect., Engl. Transl.*, *243*, 1-4, 1980.

Greenberg, J. G., and E. A. Okal, Intraplate seismicity of the southern part of the Pacific plate (abstract), *Eos, Trans. AGU*, *64*, 269, 1983.

Gutenberg, B., Earthquake energy released at various depths, *Verh. K. Ned. Geol. Mijnbouwkd. Genoot. Geol. Ser.*, *14*, 165-175, 1957.

Gutenberg, B., and C. F. Richter, *Seismicity of the Earth*, pp. 229-230, Princeton University Press, Princeton, N. J., 1954.

Hayes, D. E., and M. Ewing, The Louisville Ridge: a possible extension of the Eltanin fracture zone, in *Antarctic Oceanology I, Antarct. Res. Ser.*, vol. 15, edited by J.L. Reid, pp. 223-228, AGU, Washington, D. C., 1971.

Henderson, L. J., and R. G. Gordon, Oceanic plateaus and the motion of the Pacific plate with respect to hotspots (abstract), *Eos, Trans. AGU*, *62*, 1028, 1981.

Hey, R. N., A new class of "pseudofaults" and their bearing on plate tectonics: Propagating rift model, *Earth Planet. Sci. Lett.*, *37*, 321-325, 1977.

Hey, R. N., and D. S. Wilson, Propagating rift explanation for the tectonic evolution of the northeast Pacific -- the pseudomovie, *Earth Planet. Sci. Lett.*, *58*, 167-188, 1982.

Kanamori, H., Synthesis of long-period surface waves and its application to earthquake source studies -- Kurile Islands earthquake of October 13, 1963, *J. Geophys. Res., 75*, 5011-5027, 1970.

Kanamori, H., Seismic and aseismic slip along subduction zones and their tectonic implications, in *Island Arcs, Deep Sea Trenches and Back-Arc Basins, Maurice Ewing Ser.*, vol. 1, edited by M. Talwani and W.C. Pitman III, pp. 163-174, AGU, Washington, D. C., 1977*a*.

Kanamori, H., The energy release in great earthquakes, *J. Geophys. Res., 82*, 2981-2987, 1977*b*.

Kanamori, H., and K. Abe, Re-evaluation of the turn-of-the-century seismicity peak, *J. Geophys. Res., 84*, 6131-6139, 1979.

Kanamori, H., and G. S. Stewart, Mode of strain release along the Gibbs Fracture Zone, Mid-Atlantic Ridge, *Phys. Earth Planet. Inter., 11*, 312-332, 1976.

Lay, T., and H. Kanamori, An asperity model of large earthquake sequences, in *Earthquake Prediction, an International Review, Maurice Ewing Ser.*, vol. 4, edited by D.W. Simpson and P.G. Richards, pp. 579-592, AGU, Washington, D. C., 1981.

Mammerickx, J., S. M. Smith, I. L. Taylor, and T. E. Chase, Topography of the South Pacific, Map, Scripps Inst. Oceanogr., Univ. Calif., San Diego, 1975.

Menard, H. W., Depth anomalies and the bobbing motion of drifting islands, *J. Geophys. Res., 78*, 5128-5138, 1973.

Minster, J. B., and T. H. Jordan, Present-day plate motions, *J. Geophys. Res., 83*, 5331-5354, 1978.

Molnar, P., Earthquake recurrence intervals and plate tectonics, *Bull. Seismol. Soc. Am., 69*, 115-133, 1979.

Molnar, P., T. Atwater, J. Mammerickx, and S. M. Smith, Magnetic anomalies bathymetry, and tectonic evolution of the South Pacific since the late Cretaceous, *Geophys. J. R. astr. Soc., 40*, 383-420, 1975.

Morgan, W. J., Rodriguez, Darwin, Amsterdam,... A second type of hotpsot island, *J. Geophys. Res., 83*, 5355-5360, 1978.

Morgan, W. J., Hotspot tracks and the opening of the Atlantic and Indian oceans, in *The Sea*, edited by C. Emiliani, pp. 443-487, John Wiley, New York, 1981.

Okal, E. A., Intraplate seismicity of Antarctica and tectonic implications, *Earth Planet. Sci. Lett., 52*, 397-409, 1981.

Okal, E. A., and L. M. Stewart, Slow earthquakes along oceanic fracture zones: Evidence for asthenospheric flow away from hotspots?, *Earth Planet. Sci. Lett., 57*, 75-87, 1982.

Okal, E. A., J. Talandier, K. A. Sverdrup, and T. H. Jordan, Seismicity and tectonic stress in the Southcentral Pacific, *J. Geophys. Res., 85*, 6479-6495, 1980.

Ruff, L., and H. Kanamori, Seismicity and the subduction process, *Phys. Earth Planet. Inter., 23*, 240-252, 1980.

Sandwell, D. T., A detailed view of the South Pacific from GEOS-3 and SEASAT altimeter data (abstract), *Eos, Trans. AGU, 63*, 1120, 1982.

Schilling, J.-G., Iceland mantle plume: Geochemical study of Reykjanes Ridge, *Nature, 242*, 565-571, 1973.

Schilling, J.-G., R. Kingsley, S. E. Humphris, and G. Thompson, Ascension and St. Helena hotspots (abstract), *Eos, Trans. AGU, 63*, 474, 1982.

Sclater, J. G., L. A. Lawver, and B. Parsons, Comparison of long-wavelength residual elevation and free air gravity anomalies in the North Atlantic and possible implications for the thickness of the lithospheric plate, *J. Geophys. Res., 80*, 1031-1052, 1975.

Seismological Society of America, *Seismology Microfiche Publications From the Caltech Archives*, Ser. II and III, edited by J.R. Goodstein, H. Kanamori and W.H.K. Lee, Berkeley, Calif., 1980.

Stein, S., A model for the relation between spreading rate and oblique spreading, *Earth Planet. Sci. Lett., 39*, 313-318, 1978.

Stein, S., and G. C. Kroeger, Estimating earthquake source parameters from seismological data, in *Solid Earth Geophysics and Geotechnology*, edited by S. Nemat-Nasser, pp. 61-71, American Society of Mechanical Engineers, New York, 1981.

Stewart, L. M., Strain release along oceanic transform faults, Ph.D. thesis, Yale University, New Haven, Conn., 1983.

Stewart, L. M., and E .A. Okal, Do all transform faults exhibit m_b-M_s disparity? (abstract), *Eos, Trans. AGU, 62*, 1031-1032, 1981.

Stewart, L. M., and E. A. Okal, Intraplate events along Indian Ocean Fracture Zones make up for seismic slip required on transform faults (abstract), *Eos, Trans. AGU, 63*, 1023, 1982.

Sykes, L. R., Aftershock zones of great earthquakes, seismicity gaps, and earthquake predictions for Alaska and the Aleutians, *J. Geophys. Res., 76*, 8021-8041, 1971.

Turcotte, D. L., and G. Schubert, *Geodynamics*, 450 pp., John Wiley, New York, 1982.

Vink, G. E., and W. J. Morgan, Iceland-Faeroe Plateau: A hotspot-fed ridge (abstract), *Eos, Trans. AGU, 62*, 382, 1981.

Vogt, P. R., Plumes, subaxial flow, and topography along the mid-oceanic ridge, *Earth Planet. Sci. Lett., 29*, 309-325, 1976.

Vogt, P. R., and G. L. Johnson, Transform faults and longitudinal flow below the mid oceanic ridge, *J. Geophys. Res., 80*, 1399-1428, 1975.

Weissel, J. K., D. E. Hayes, and E. M. Herron, Plate tectonics synthesis: The displacements between Australia, New Zealand, and Antarctica since the late Cretaceous, *Mar. Geol., 25*, 231-277, 1977.

Wiens, D. A., and S. Stein, Age dependence of oceanic intraplate seismicity and implications for lithospheric evolution, *J. Geophys. Res., 88*, 6455-6468, 1983.

L. M. Stewart, Department of Geological Sciences, Brown University, Providence, Rhode Island 02912.

E. A. Okal, Department of Geology and Geophysics, Yale University, Box 6666, New Haven, Connecticut 06511; as of Jan. 1, 1984: Department of Geological Sciences, Northwestern University, Evanston, Illinois 60201.

(Received November 9, 1982;
revised May 6, 1983;
accepted June 16, 1983.)